Tsunami Hazard Modelling in Sunda Strait, West Java, Indonesia

Mauliza Fatwa Yusdian, Aditya Saputra, Kuswaji Dwi Priyono, Vidya Nahdhiyatul Fikriyah, Afif Ari Wibowo, Mika Yoshida and Namiko Sano

January 6, 2025

Available online at www.sciencedirect.com

ScienceDirect

Transportation Research Procedia 00 (2021) 000–000

Transportation Research Procedia

www.elsevier.com/locate/procedia

The 1st International Conference on Smart Mobility and Logistics Ecosystems (SMiLE)

September 17-19, 2024, KFUPM, Saudi Arabia

TSUNAMI HAZARD MODELLING IN SUNDA STRAIT, WEST JAVA, INDONESIA

Mauliza Fatwa Yusdian[a], Aditya Saputra[a*], Kuswaji Dwi Priyono[a], Vidya Nahdhiyatul Fikriyah[a-b], Afif Ari Wibowo[a], Mika Yoshida[c], Namiko Sano[c]

[a]*Geography Faculty, Universitas Muhammadiyah Surakarta, Central Java, Indonesia*
[b]*Natural Resource Department, University of Twente, The Netherlands*
[c]*Graduate School of Maritime Science, Kobe University, Japan.*

Abstract

The Sunda Strait is one of the tsunamigenic regions in Indonesia and is part of the Sunda Megathrust, known to be highly vulnerable to earthquakes and tsunamis. The maximum earthquake in the Sunda Megathrust can reach 8.2-8.7 Mw. This research examines the tsunami hazard in Cilegon City, Banten, Indonesia, which directly borders the Sunda Strait. The purpose of this study is to determine the tsunami wave *run-up* height and analyse the inundation area due to tsunami waves in Cilegon City. The methods used in this research include tsunami modelling with three earthquake scenarios of magnitudes 8.2 Mw, 8.45 Mw, and 8.7 Mw using COMCOT *software* and H-loss calculations. Based on the results of the tsunami hazard analysis in Cilegon City using a geographic information system involving COMCOT *software* and H-loss calculations, the tsunami hazard in Cilegon City is relatively low. The wave arrival time at the Cilegon City coast from each scenario is 141.9 minutes, 150 minutes, and 84.2 minutes respectively, with *run-up* heights not exceeding 3 meters and inundation areas less than 200 hectares in the Ciwandan, Citangkil, and Grogol Districts.

Keywords: Tsunami Hazard; Cilegon City; Sunda Megatrust; COMCOT

1. Introduction

The Sunda Strait is a tsunamigenic region in Indonesia (Yudhicara and K. Budiono, 2008). One of the reasons is the presence of the subduction zone from western Sumatra to southern Java, known as the Megathrust. The earthquake threat in the Megathrust zone of the Sunda Strait ranges from 8.2 to 8.7 Mw (Irsyam et al., 2010). The following (Fig.1) is a map of segmentation and maximum magnitude of subduction in Indonesia in 2017.

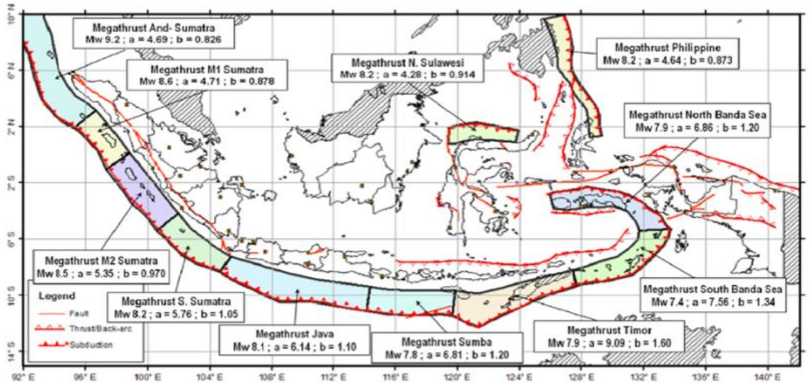

Fig.1 Model of subduction and earthquake source (Megathrust) in Indonesia (Irsyam et al., 2010)

The Sunda Strait Megathrust can trigger thousands of earthquakes centered around the plate subduction zone and can invite secondary disasters such as tsunamis. The destructive impacts of tsunami disasters are detrimental to various aspects of life. The Sunda Strait tsunami on December 22, 2018, caused by volcanic activity at Anak Krakatau, resulted in landslides of material from Anak Krakatau into the sea. This event caused damage in the districts of Serang and Pandeglang, Banten Province, as well as in the districts of Tanggamus, Pesawaran, and South Lampung, Lampung Province. According to tempo.co, Vindry Florentin (2019) wrote on his website www.nasional.tempo.com, that the National Disaster Management Agency (BNPB) stated that there were approximately 437 fatalities, 1,459 injuries, and 10 missing persons.

Cilegon City is an industrial city directly bordering the Sunda Strait, thus being a tsunami-prone area. The impact of a tsunami in the industrial area of Cilegon City is feared to invite secondary disasters in the form of technological failures such as the spread of hazardous chemicals that could threaten the community (BNPB, 2012). The coastal areas of Cilegon City are vital areas, with many infrastructures supporting the population's centers of activity such as industry, economy, and tourism. Therefore, it is important to conduct research on tsunami hazard analysis in Cilegon City as a form of disaster mitigation to reduce the resulting disaster impacts.

Tsunami hazard analysis with tsunami modeling is expected to accurately model tsunamis according to actual conditions, thus producing accurate inundation estimates. Numerical models in tsunami modeling are used to determine tsunami wave *run-up* heights and inundation areas accurately. The use of Geographic Information Systems (GIS) can provide objective and up-to-date information. This research uses COMCOT *software* version 1.7 to model *near-field* tsunamis generated by seabed deformations based on *Shallow Water Equations* applying a *leap-frog* scheme with a multi-grid system up to 12 *sub-level grids* (Wang, 2009). The multi-grid system allows for the use of multiple simulation areas to improve modeling accuracy and efficiency. Additionally, GIS is capable of integrating natural phenomena with other aspects such as demographics, social, economic, and others, thus supporting research as an ideal assessment tool.

2. Method

The research methodology used is a quantitative analysis method utilizing numerical modeling software COMCOT version 1.7 based on Shallow Water Equations with a leap-frog scheme using a multi-grid system (Wang, 2009) and H-loss calculations (Berryman, 2006 in BNPB, 2016). The COMCOT software is used to determine run-up values, while H-loss calculations are used to determine inundation areas. The population in this study is the affected areas in the Cilegon City region, which are sampled using the Stratified Sampling Method determined based on the distance levels of the sample points to the earthquake epicenter in the Sunda Strait Megathrust. Figure 2 shows the map of sample point locations.

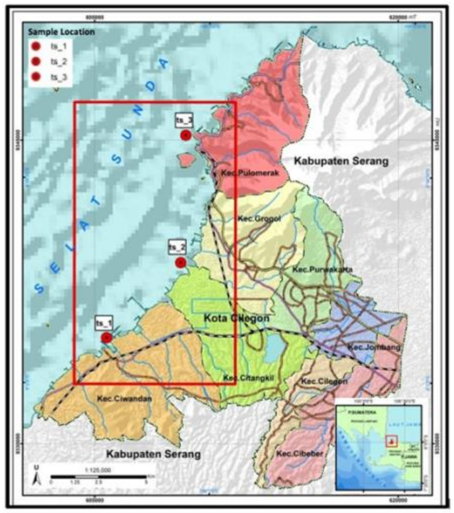

Fig. 2 Sample Location

The data used in this study are secondary data such as earthquake data, fault parameter, bathymetry data, topography data, land use and land cover, coastline data, and MSL (mean sea level). Those data were obtained from various credible institution both national and overseas. The summary of data needed, can be seen in Table 2.

Table 1. List of data needed

Data	Source	Function
Earthquake data (1977-2019)	USGS	Seismic Hazard
Fault Parameter	Global CMT	Tsunami Source Modelling
Bathymetry	National Geo-Spatial Agency	Tsunami propagation model
Topography	National Geo-Spatial Agency	Run-Up Tsunami
Land use	Local government	Hazard modelling
Coastline	National Geo-Spatial Agency	Run-up Tsunami
MSL	Catherinna et al. in 2015	Run-up Tsunami

Fault parameter data taken from the Global Centroid Moment Tensor (Global CMT) based on historical earthquakes. This data consists of fault parameters used as a reference for earthquake scenario creation. The selection of earthquake epicenters is based on thrust fault earthquakes closest to the research location. Thrust fault earthquakes are combined with the maximum Magnitude (Mw) from the Indonesian earthquake book for the Sunda Strait Megathrust in 2010 (8.2 Mw) and 2017 (8.7 Mw), as well as the average scenario on the Sunda Strait Megathrust (8.45 Mw). The data processing technique involves several stages, including calculating fault parameters and determining grids for tsunami modeling scenarios, as well as determining roughness coefficients for H-loss calculations. Fault parameters such as strike, dip, M, slip, and depth were obtained from the Global CMT website. However, some fault parameters such as length, width, and fault area need to be calculated using formulas. The calculation of the length and width of deformation can be determined based on the Papazachos et al. equation (2004). To calculate length, width, and fault in the dip-slip type, the equations are as follows:

$$\text{Log } L = 0.55\,M - 2.19 \quad (1)$$

$$\text{Log } W = 0.31\,M - 0.63 \quad (2)$$

$$\text{Log } S = 0.86\,M - 2.82 \quad (3)$$

$$\text{Log } u = 0.64\,M - 2.78 \quad (4)$$

Where L is rupture length (km); W is rupture width (km); S is rupture area (km2); u is average displacement (cm)

Tsunami modeling is conducted using COMCOT software with input fault parameters. The following are the earthquake scenarios used in the study (Table 2). The creation of a Nested Grid or hierarchical grid involves grids of different sizes to represent wave profiles in detail in shallow water areas during tsunami modeling. Fig 3 shows the grid sizes used in the study.

Table 2. The fault parameter

Fault	1	2	3
Latitude (°LS)	-7.23	-7.23	-7.23
Longitude (°BT)	103.76	103.76	103.76
Length (km)	209	287	394
Width (km)	82	98	117
Displacement/slip (m)	2.93	4.25	6.14
Magnitude (Mw)	8.2	8.45	8.7
Strike (°)	112	112	112
Dip (°)	50	50	50
Slip (°)	81	81	81
Depth (km)	15 15	15	15

Source: Historical earthquakes data from USGS and BMKG, Papazachos et al. (2004), Global CMT fault parameters, Indonesian Earthquake Book (2010 and 2017).

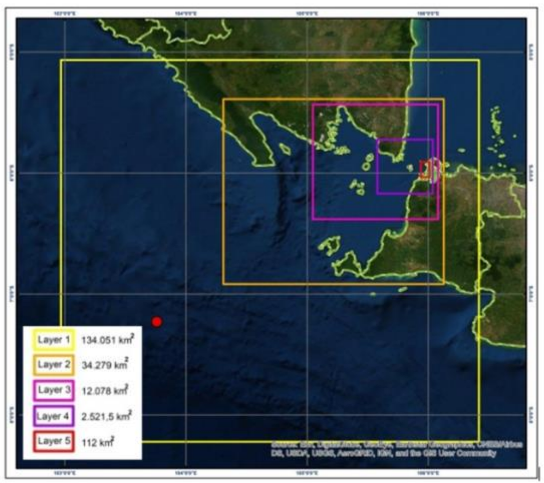

Fig. 3 Hierarchical grid In Tsunami modelling

Tsunami modeling using COMCOT software can be continued by inputting fault parameters and bathymetry layers into comcot.ctl. Tsunami modeling for each scenario is conducted for 2 hours and 30 minutes (9000 seconds). The resulting data includes run-up height and wave arrival time. The run-up height data obtained is used as input for H-loss calculations to determine the inundation area due to the earthquake. This research utilizes analysis from Berryman, which serves as a reference in Regulation No. 2 of BNPB in 2012, the National Guidelines for Tsunami Disaster Risk Assessment. Berryman establishes coefficient values based on land cover or land use types, as follows:

Table 3. Land cover coefficient value

Land Cover/Land Use Type	Coefficient Value (n)	
	n	n^2
Water Bodies	0.007	0.000049
Shrubland	0.040	0.0016
Forest	0.070	0.0049
Plantation	0.035	0.001225
Open Empty Land	0.015	0.000225
Agricultural Land	0.025	0.000625
Settlements/Built-Up Areas	0.045	0.002025
Mangrove	0.025	0.000625
Fishponds/Ponds	0.010	0.0001

Source: Berryman, 20016

Modeling the distribution of tsunami-affected areas refers to Regulation No. 2 of BNPB regarding the National Guidelines for Tsunami Disaster Risk Assessment. H-loss calculation is obtained from the mathematical equations developed by Berryman based on the calculation of tsunami height loss per 1 m distance of inundation (flood height) based on distance values to the slope and surface roughness (BNPB, 2016). The following is the equation for H-loss calculation

$$Hloss = \left(\frac{167\, n^2}{Ho^{\frac{1}{3}}}\right) + 5\, sinS \quad (5)$$

Where: H Loss is tsunami height loss per 1 m distance of inundation; n^2 is surface roughness coefficient; $H_o^{1/3}$ is tsunami wave height at the shoreline (m); and s is slope angle (degrees).

3. Results and Discussion

This study employs five grids as modeling media for bathymetric data and wave propagation speed from the earthquake epicenter to the coastal edge sampling points in Cilegon City. The grids are created according to the functions required during the modeling process. The first grid represents layer 1, determined by considering the earthquake epicenter area and sampling point locations. The second to fourth grids encompass the Sunda Strait region, allowing for a more detailed representation of waves passing through small islands in the Sunda Strait area. The last grid is layer 5, representing waves at the sampling points. This grid covers the coastal areas of Cilegon City and plays a crucial role as the endpoint for wave propagation in shallow water. Grid division is an essential element in modeling tsunamis triggered by earthquakes. Grids delineate deep and shallow waters, which trigger changes in wave velocity. Grid division and visualization of bathymetry on grids showing depth differences can be seen in Fig.4.

The earthquake triggering the tsunami is caused by a reverse fault earthquake with a significant angle (Pawirodikromo, 2012). The mechanism of the reverse fault in the scenario is characterized by the initial conditions of the earthquake (at minute 0), which cause the deformation of the fault plane leading to the lowering of the sea surface. The fault plane's lowering occurs in the northern part of the sea facing the Sunda Strait, resulting in a decrease in the sea surface near the earthquake epicenter's coast, while a rise in the sea surface occurs facing the Indian Ocean. The initial conditions of the tsunami modeling results in each scenario differ, which is due to the varying strength of the earthquakes. The initial conditions of the tsunami caused by earthquakes in the Sunda Strait Megathrust can be seen in the following Fig. 5. The magnitude of the earthquake influences the extent of wave propagation, which affects the speed of wave propagation. A common difference is observed in the wave arrival time at each scenario's sampling point. Meanwhile, the distance and slope conditions of the coastal slope affect the wave run-up height. A comparison of the results in terms of wave arrival time and wave run-up height in Cilegon City from the three scenarios can be seen in Fig. 9 and 10.

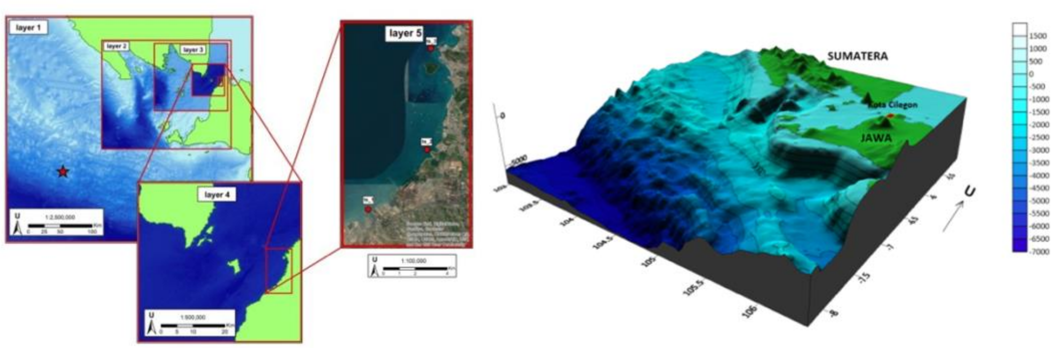

Fig 4. (Left) Grid division; (Right) Bathymetry

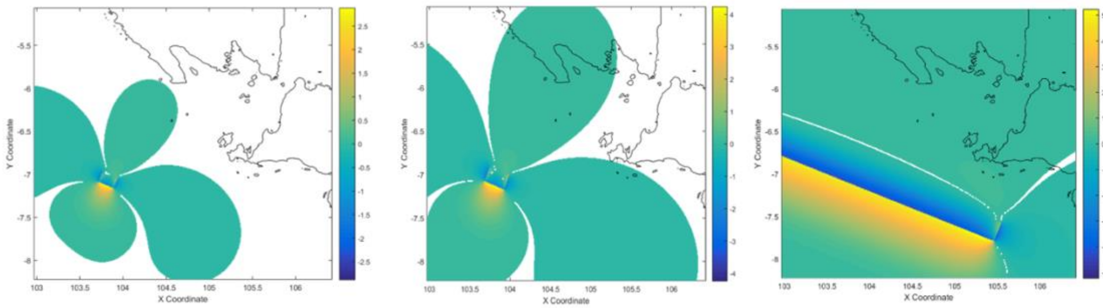

Fig. 5 (left) Result plot of *initialDisplacement* for an earthquake with a magnitude of 8.2 Mw using MATLAB; (Center) Result plot of *initialDisplacement* for an earthquake with a magnitude of 8.45 Mw using MATLAB; (right) Result plot of *initialDisplacement* for an earthquake with a magnitude of 8.7 Mw using MATLAB

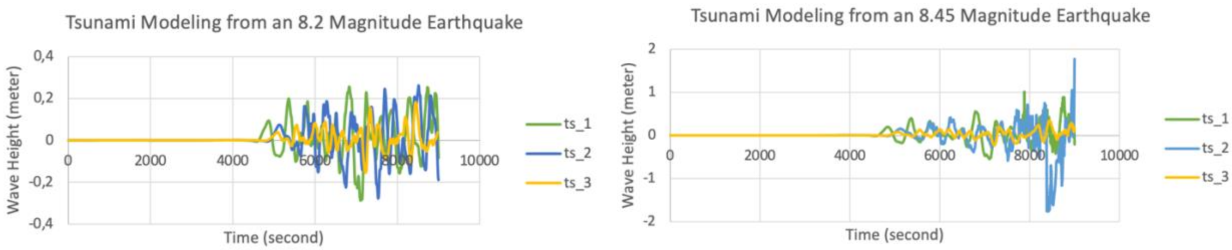

Fig 9. (Left) Tsunami Modeling Graph from an 8.2 Mw Earthquake; (right) Tsunami Modeling Graph from an 8.45 Mw Earthquake

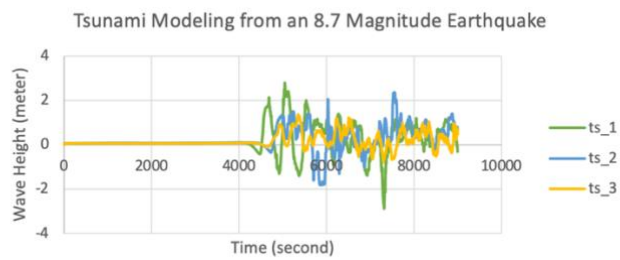

Fig. 10 Tsunami Modeling Graph from an 8.7 Mw Earthquake.

The scenarios used in this study utilize three sampling points functioning as *tide gauges* to record waves. Tsunami modeling in each scenario resulted in average *run-up* heights of 0.236 m for scenario 1, 1.041 m for scenario 2, and 2.174 m for scenario 3. Tsunami hazards vary across scenarios with different earthquake strengths, both in terms of wave *run-up* height and arrival time. Scenario 1 produced the highest *run-up* of only 0.264 m recorded to arrive at 141.9 minutes (2 hours 21 minutes) at sampling point 2, located approximately 283.355 km from the earthquake epicenter. This differs from scenario 2, which yielded a *run-up* height of 1.774 m and arrived in 150 minutes (2 hours) at sampling point 2 at the same distance from the earthquake epicenter. In scenario 3, the resulting run-up height is 2.802 m at sampling point 1, arriving in the fastest time of 84.2 minutes (1 hour 24 minutes) at a distance of 277.433 km. The arrival time and wave *run-up* height for each scenario can be detailed in Tables 4, 5, and 6.

Table 4. Arrival Time and Wave Height of Scenario 1.

Earthquake Scale	**Time**		**First Wave (meter)**	**Time**		**Wave Peak (meter)**
(8.2)	**Second**	**Minutes**		**Second**	**Minute**	
ts_1	4.869	81,2	0,095	6.830	113,8	0,259
ts_2	5.130	85,5	0,075	8.516	141,9	0,264
ts_3	5.080	84,7	0,039	8.444	140,7	0,184
Total			0,208			0,707
Average			0,069			0,236

Table 5. Arrival Time and Wave Height of Scenario 2

Earthquake Scale (8.2)	Time Second	Time Minutes	First Wave (meter)	Time Second	Time Minute	Wave Peak (meter)
ts_1	4842	80,7	0,199	7883	131,4	1,014
ts_2	5130	85,5	0,157	9000	150,0	1,774
ts_3	5073	84,6	0,081	8458	141,0	0,334
Total			0,437			3,122
Average			0,146			1,041

Table 6. Arrival Time and Wave Height of Scenario 3

Earthquake Scale (8.2)	Time Second	Time Minutes	First Wave (meter)	Time Second	Time Minute	Wave Peak (meter)
ts_1	4.687	78,1	2,154	5.050	84,2	2,802
ts_2	4.897	81,6	1,135	7.531	125,5	2,353
ts_3	4.929	82,2	0,931	5.353	89,2	1,368
Total			4,220			6,522
Average			1,407			2,174

The study area, located in a strait with the research site far from the earthquake epicenter, affects the modeling results. This is due to the strait being shallow waters that will slow down the wave propagation speed, resulting in longer wave arrival times compared to locations near deep waters or directly bordering the ocean. The Sunda Strait region, which is the focus of the study, also has many small islands like the volcanic Anak Krakatau and other islands that will influence the waves. This can be observed from the modeling results graph, which shows that the highest waves do not occur in the first wave. The incoming waves will be reflected by small islands like Pulau Sangiang, causing high waves to occur repeatedly over a long period. The numerical modeling conducted yielded wave arrival times and run-up heights used in the H-loss calculation. The H-loss calculation combines the average run-up height with the conditions of Cilegon City as parameters. These conditions include the slope inclination, land use, and surface roughness coefficient in Cilegon City. The slope inclination data used in this calculation are from the National DEM website BIG. Land use data comes from the Cilegon City Planning Agency (BAPPEDA) in 2015, used to calculate the surface roughness coefficient

Scenario 1, with an average run-up height of 0.236 m, resulted in an inundation area of 0.6625 ha. Scenario 2 produced a larger inundation area than Scenario 1, covering 43.1690 ha with an average run-up height of 1.041 m. Scenario 3 had the widest inundation area of the three scenarios, with a run-up height of 2.174 m, resulting in an area of 138.2708 ha. The inundation area extends along the coastline of Cilegon City. The inundation area is visualized with a tsunami inundation map focusing on sample points 1 and 2, considering the highest run-up value at these points, the distance of the sample points from the earthquake epicenter, and the land use in Cilegon City.

The selection of focus locations considers the highest run-up values at each sample point, always occurring at points 1 and 2. Additionally, the distance of the sample points from the earthquake epicenter and the land use in Cilegon City are crucial considerations. The land use around sample points 1 and 2 in Cilegon City consists of built-up areas dominated by industrial zones. In sample point area 1, there is the PT Krakatau Bandar Samudera port, an import and export port, and PT Krakatau Steel, a state-owned enterprise (BUMN) engaged in the national steel industry. Sample point 1 is located in the Ciwandan District, which has the shortest distance from the earthquake epicenter, approximately 277.433 km away. On the other hand, in sample point area 2, there is the PT Krakatau Daya Listrik power plant complex, which serves as a power plant to meet the high electricity demand, with PT Krakatau Steel as its main consumer. Additionally, there is a fuel depot owned by Pertamina. Sample point 2 appears twice as the recipient of the highest waves, as this area has a slope inclination ranging from 0 to 8%. The presence of mangrove forests on the coast of the Citangkil District and river estuaries on the coast of the Grogol District proves that the slope inclination in the sample point 2 area is very low

The inundation distribution in each district differs due to differences in the length of the coastline. The inundation area in Ciwandan District for each scenario, with a percentage comparison of the total inundation area, is 0.1674 ha (25%), 16.3655 ha (38%), and 46.4535 ha (34%), respectively. In Citangkil District, the inundation area for each scenario, with a percentage comparison of the total inundation area, is 0.2049 ha (31%), 2.5502 ha (6%), and 32.9084 ha (24%), respectively. In Grogol District, the inundation area for each scenario, with a percentage comparison of the total inundation area, is 0.0356 ha (5%), 6.0104 ha (14%), and 13.5687 ha (10%), respectively. The inundation distribution in scenario 1 is centered at sample point 2, as evidenced by the percentage of the total inundation area in Citangkil and Grogol Districts, which is 36%. In contrast, in scenario 2, the inundation area is centered at sample point 2, specifically on the coast of Ciwandan District, with a percentage of 38%. Similarly, in scenario 3, the largest inundation area is in Ciwandan District, accounting for 34% of the total inundation area.

In addition to the influence of coastline length, differences in inundation areas are also influenced by slope and land use. In Scenario 1, the highest percentage of inundation area is at sample point 2 due to the low slope inclination in the Citangkil and Grogol Districts, combined with a mix of built-up and non-built-up land use, allowing for sandy beaches that enable waves to reach the shore. The presence of Pulau Sangiang also affects wave reflections, causing waves to arrive multiple times at sample point 2. The percentage of inundation area in Scenarios 2 and 3 is more dominant in the Ciwandan District, specifically at sample point 1. This is influenced by the proximity of the Ciwandan District to the earthquake epicenter and the higher run-up heights in Scenarios 2 and 3 compared to Scenario 1. Although most of the coastal areas in the Ciwandan District have been developed, allowing waves to reach and flood the PT Krakatau Bandar Samudera port. At sample point 2, particularly in the Citangkil District, the inundation in Scenario 3 is seen in the mangrove forests and coastal areas with industrial and agricultural zones. The distribution of inundation in Cilegon City can be seen in detail on the tsunami inundation maps in Figures 11, 12, and 13

4. Conclusion

The tsunami modeling results using COMCOT software show that the tsunami hazard in Cilegon City is relatively low, as the run-up values generated are less than 3 meters, which is the threshold set by the National Disaster Management Agency in Regulation No. 2 of 2012, the National Guideline for Tsunami Disaster Risk Assessment. This can be seen from the highest run-up and arrival times in scenario 1 of 0.264 m in 141.9 minutes (1 hour and 21 minutes), scenario 2 of 1.041 m in 150 minutes (2 hours), and scenario 3 of 2.174 m in 84.2 minutes (1 hour and 24 minutes). The tsunami modeling results show that the average run-up height from each sample point in each scenario respectively is 0.236 m, 1.041 m, and 2.174 m. The total inundation area generated in each scenario is less than 200 ha. The inundation areas for each scenario, respectively, are 0.6625 ha, 43.1690 ha, and 138.2708 ha, with varying inundation areas in each district. The inundation area in Ciwandan District for each scenario, respectively, is 0.1674 ha, 16.3655 ha, and 46.4535 ha. The inundation areas in Citangkil District for each scenario, respectively, are 0.2049 ha, 2.5502 ha, and 32.9084 ha. The inundation areas in Grogol District for each scenario, respectively, are 0.0356 ha, 6.0104 ha, and 13.5687 ha.

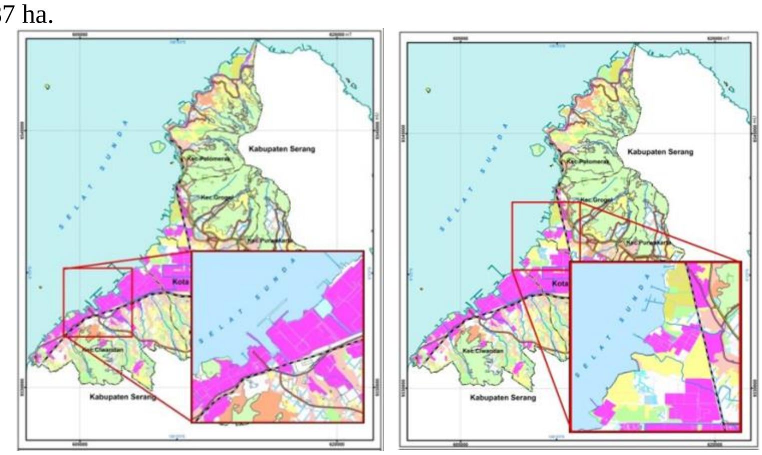

Fig. 11 (Left) Tsunami Hazard Map Due to 8.2 Mw Earthquake in Ciwandan District; (Right) Tsunami Hazard Map Due to 8.2 Mw Earthquake in Citangkil and Grogol Districts

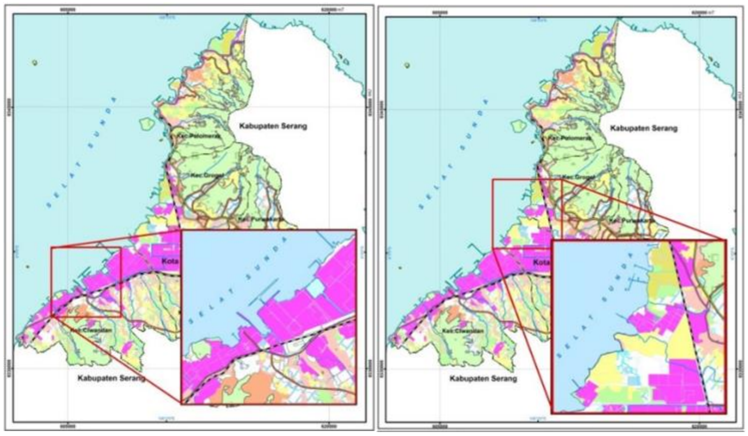

Fig. 12 (Left) Tsunami Hazard Map Due to 8.45 Mw Earthquake in Ciwandan District; (Right) Tsunami Hazard Map Due to 8.45 Mw Earthquake in Citangkil and Grogol Districts

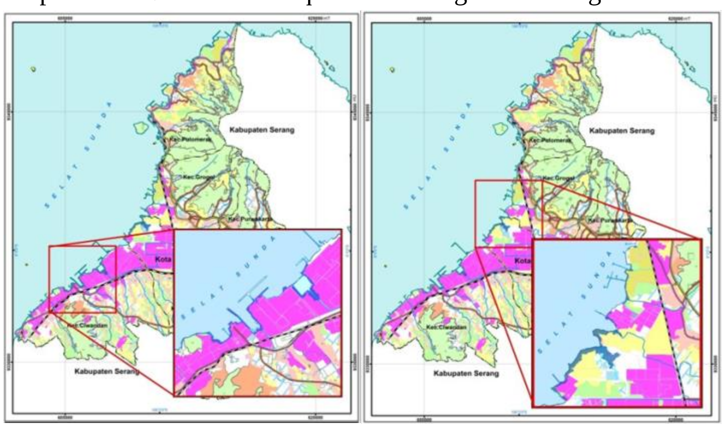

Fig. 13 (Left) Tsunami Hazard Map Due to 8.7 Mw Earthquake in Ciwandan District; (Right) Tsunami Hazard Map Due to 8.7 Mw Earthquake in Citangkil and Grogol Districts

Acknowledgements

The authors are thankful to Geography Faculty, Universitas Muhammadiyah Surakarta who has provided adequate tool and supported this project.

References

Catherinna, et al. (2015). Bathymetric Mapping of Anyer Waters, Banten Using Multibeam Echosounder System (MBES) *Journal of Oceanography*, vol. 4, no. 1, 2018, pp. 253-261 from: *http://ejournal-s1.undip.ac.id/index.php/jose*, [April 20, 2020].

Irsyam, M., Sengara, I.W., Aldiamar, F., Widiyantoro, S., Triyoso, W., Natawidjaja, D.H., Kertapati, E., Meilano, I., Suhardjono, Asrurifak, M., Ridwan, M. (2010). Ringkasan hasil studi tim revisi peta gempa Indonesia 2010. Retrieved from http://www.preventionweb.net/files/14654_AIFDR.pdf.

National Disaster Management Agency. (2012). *Towards Indonesia Resilient Facing Tsunami*. [online], from: *www.bnpb.go.id* [September 1, 2019].

National Disaster Management Agency. (2016) *Disaster Risk Indonesia*. [online], from: *www.bnpb.go.id* [September 1, 2019].

National Seismic Study Center. (2017) *National Seismic Book 2017*. [online], from: *www.litbang.pu.go.id* [September 5, 2019].

National Seismic Study Center. (2010) *National Seismic Book 2010*. [online], from: *www.litbang.pu.go.id* [September 5, 2019].

Pawirodikromo W. (2012). *Engineering Seismology Seismology. Yogyakarta*: Pustaka Pelajar.

Papazachos, et al. (2004). Global Relations Between Seismic Fault Parameters And Moment Magnitude of Earthquakes. *Proceedings of the 10th International Congress Thessaloniki*, vol. 36, no. 17 April 2004, pp. 1482-1489 [online], from: *https://www.researchgate.net/publication/260200287_Global_relations_between_seismic_fault_parameters_and_moment_magnitude_of_earthquakes/link/575158f908ae17e65ec14c80/download* [September 20, 2019].

Yudhicara and K. Budiono. (2008) Tsunamigenic In the Sunda Strait: A Study of Soloviev Tsunami Catalog. *Journal of Indonesian Geology*, vol. 3, no. 4 December 2008, pp. 241-251, from: *www.researchgate.net*, [August 25, 2019].

Wang. (2009). *User Manual For COMCOT Version 1.7*. New York: Cornell University [online], from: *http://citeseerx.ist.psu.edu/viewdoc/download?doi=10.1.1.512.84&rep=rep1&type=pdf* [December 20, 2019].